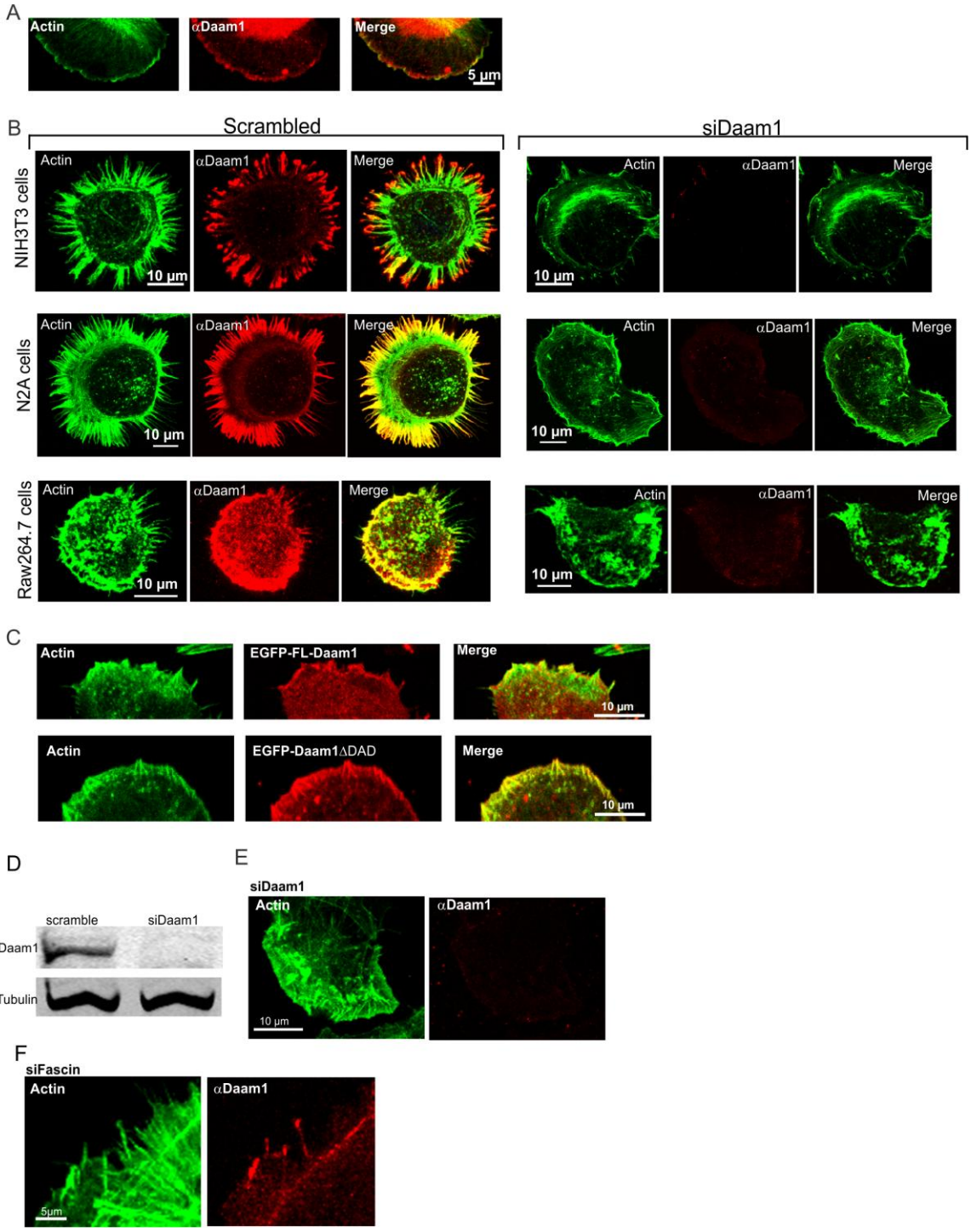

Figure S1. Immunolocalization and RNAi silencing of Daam1 in multiple cell lines. (**A**) Immunolocalization of endogenous Daam1 in B16F1 cells detected with a different α-Daam1 antibody (kind gift from Ray Habas) from the K-16 α-Daam1 antibody used in Figure 1. (**B**) Immunolocalization and silencing of Daam1 in NIH3T3 fibroblasts (top row), N2A neuroblastoma cells (middle row), and Raw264.7 macrophages (bottom row). Daam1 was localized using the K-16 α-Daam1 antibody. Actin was stained with rhodamine phalloidin. (**C**) Immunolocalization of EGFP-Daam1 constructs in fixed B16F1

cells using α-GFP antibodies. EGFP-FL-Daam1 and EGFP-Daam1ΔDAD both localize to lamellipodia and filopodia. (**D**) Western blot analysis of cells treated with scramble siRNA oligos and siDaam1 oligos. 10 µg of each cell lysate was fractionated on a 12.5% SDS-PAGE gel, blotted and probed with the K-16 α-Daam1 antibody. Blots were probed with α-tubulin antibody as a loading control. (**E**) B16F1 cells after Daam1 silencing were stained with rhodamine phalloidin (left) and K-16 α-Daam1 antibody (right). (**F**) Silencing of fascin diminishes Daam1-localization to filopodia shafts but not tips.

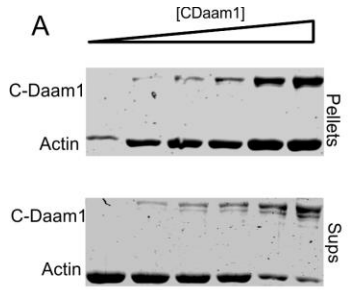

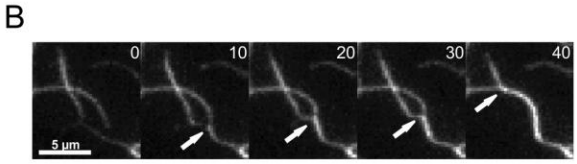

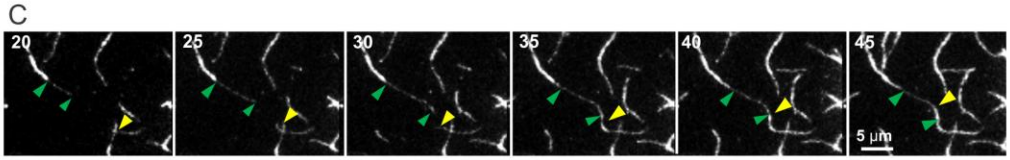

D

	F-actin + Fascin	F-actin + Daam1	F-actin + Daam1 + Fascin
Bundle organization	Rigid, straight and flat*	Flexible, wavy, rounded* and consist of sub-bundles	Semi-flexible, inter-mediate rounded,partly flat
Organization of filaments within bundles	Straight, evenly spaced and aligned in parallel	Wavy, densely packed, less evenly spaced and lacking organization	Intermediate in filament spacing and organization
Number of filaments in bundles	17.7 ± 1.6	ND#	24.0 ± 1.0
Bundle width	145 ± 4 nm	268 ± 17 nm	188 ± 39 nm
Distance between filaments	8.2 ± 0.5 nm	ND#	8.2 ± 0.8 nm
Transverse repeat	36.6 ± 0.6 nm	ND#	36.6 ± 2.2 nm
	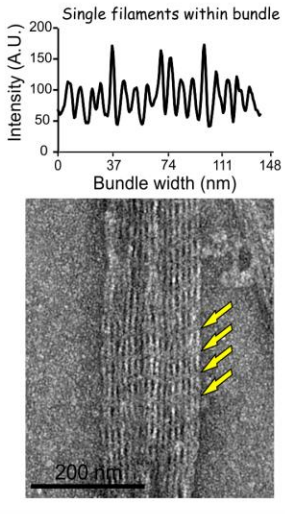	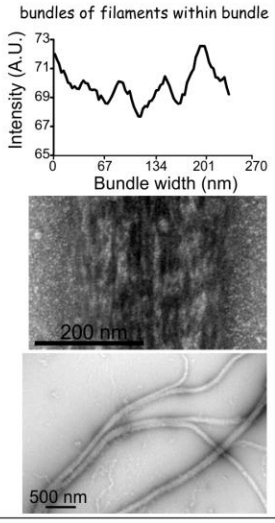	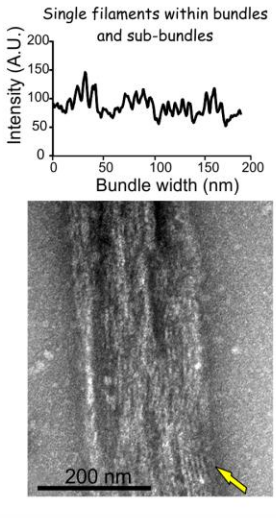

Figure S2

Figure S2. Properties of actin bundles formed by CDaam1 and fascin.
(**A**) Coomassie-stained gels showing the pellets (top) and supernatants (bottom) after low-speed pelleting of F-actin in the presence of different concentrations of CDaam1. (**B**) TIRF microscopy time-lapse imaging of rapid single actin-filament zippering-events (arrow) in the presence of 300 nM CDaam1. (**C**) Example of time lapse TIRF imaging to determine orientation of filaments in bundles, quantified in Figure 2E. 1 µM actin (10% OG-labeled) was polymerized in presence of 300 nM CDaam1 and 3 µM profilin. Green arrowheads indicate growing barbed ends of parallel oriented filaments in a bundle. Yellow arrowhead indicates a barbed end merging with the bundle in an anti-parallel fashion. Time is indicated in sec. (**D**) Ultrastructural properties of actin filament bundles formed in vitro by mixing F-actin with CDaam1, fascin, or CDaam1 and fascin together. Error bars represent SD. (*) Flatness and roundedness of bundles was indicated by the shadows from negative staining. (#) Several properties of CDaam1-generated bundles, including number of filaments per bundle, inter-filament distances, and transverse repeats, were not determined (ND) because the filaments in these bundles were too densely packed and lacked regular organization. Yellow arrows indicate periodic transverse repeats on bundles formed in the presence of fascin, which may represent regularly spaced crosslinks between filaments. Graphs show the intensity profiles, in which individual filaments in fascin bundles, and sub-bundles within CDaam1 bundles can be discerned. In the bundles formed by fascin and CDaam1 together, both individual filaments and sub-bundles are evident in the intensity profiles.

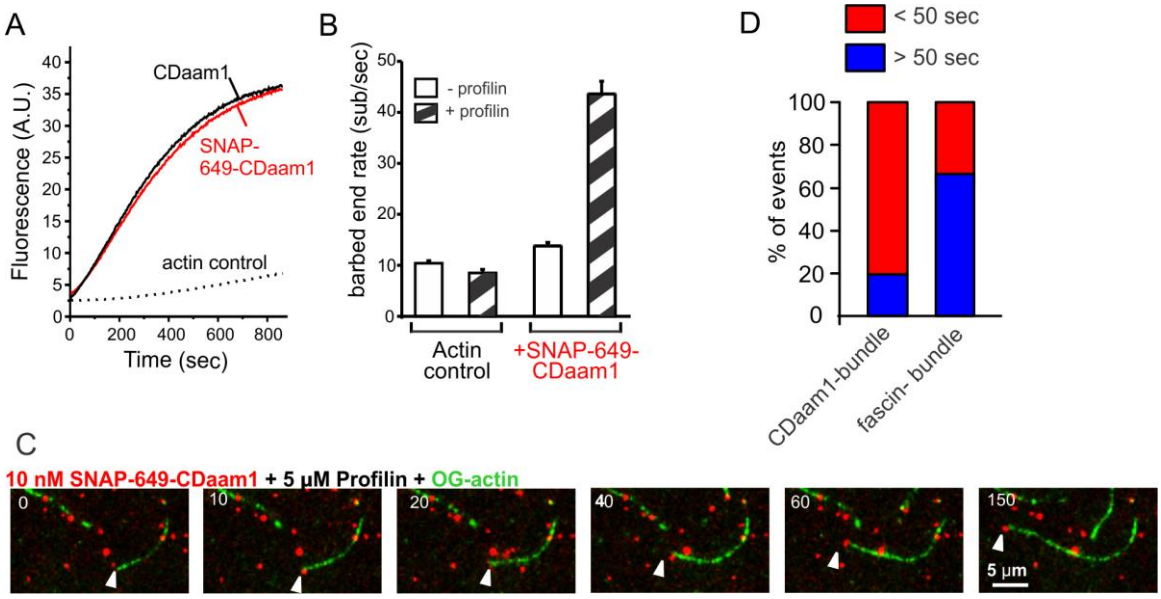

Figure S3. Biochemical activities of fluorescently labeled SNAP-649-CDaam1 molecules.

(**A**) Assembly of 2 µM G-actin (5% pyrene-labeled) in the presence of 20 nM CDaam1 or SNAP-649-CDaam1. (**B**) Quantification of elongation rates of filaments processively capped by SNAP-649-CDaam1 molecules in the presence or absence of 3 µM profilin and 1 µM actin (10% OG-labeled). Data are from experiments as in Figure 3C (n>20 filaments). Error bars indicate SD. (**C**) Example of time lapse TIRF single-molecule imaging of processive filament elongation by a SNAP-649-CDaam1 molecule (white arrowhead). Reactions contain 1 µM actin (10% OG-labeled), 3 µM profilin, and 10 nM SNAP-649-CDaam1. Time is indicated in sec in each panel. (**D**) Comparison of dwell-time distributions of SNAP-649-CDaam1 molecules on actin filament bundles generated by unlabelled CDaam1 or fascin.

SUPPLEMENTAL MOVIE LEGENDS

Movie S1. (**Left**) **Polymerizing actin filaments zippering into bundles.** 1 μM OG-actin (10% labeled) was polymerized in the presence of 300 nM CDaam1 and 5 μM profilin. The video is displayed at 12 fps and corresponds to Figure S2B. (**Right**) **CDaam1 preferentially bundle actin filaments in a parallel orientation.** 1 μM OG-actin (10% labeled) was polymerized in the presence of 300 nM CDaam1 and 5 μM profilin. Green arrows mark filament barbed ends growing in the same direction, yellow arrows mark a filament barbed end merging with a bundle in anti-parallel orientation. The video is displayed at 12 fps and corresponds to Figure S2C. Scale bars represent 10 μm.

Movie S2. Bundling of pre-formed actin filaments by CDaam1. 1 μM OG-actin (10% labeled) was polymerized in a flow chamber for 10 minutes. 300 nM of CDaam1 was flowed in after 30 sec of recording. The video is displayed at 12 fps and corresponds to Figure 2F.

Movie S3. Processive movement of fluorescently labeled SNAP-649-CDaam1 molecules on actin filament barbed ends. 1 μM OG-actin (10% labeled; green) was polymerized in the presence of 10 nM SNAP-649-CDaam1 (red) and in the absence (**left**) and presence of 5 μM profilin (**right**). The videos are displayed at 12 fps and correspond to Figure 3C and S3C. Scale bars represent 2 μm.

Movie S4. Binding of fluorescently labeled SNAP-649-CDaam1 molecules to actin filament bundles generated by CDaam1 or fascin. Bundles were first formed by incubating 1 μM actin and 5 μM profilin with 300 nM unlabeled CDaam1 or 300 nM fascin under actin polymerization conditions. After 15 min, a solution containing 300 nM unlabeled CDaam1 (left) or 300 nM fascin (right) and 1 nM SNAP-649-CDaam1 (but lacking actin monomers) in TIRF buffer was introduced to the flow channel. Videos are displayed at 24 fps. Movies correspond to Figure 4A and 4B. Scale bars represent 5 μm.

Movie S5. Diffusion of fluorescently labeled SNAP-649-CDaam1 molecules on actin filament bundles generated by unlabelled CDaam1. Bundles were first formed by incubating 1 μM actin and 5 μM profilin with 300 nM unlabeled CDaam1 under actin polymerization conditions. After 15 min, a solution containing 300 nM unlabeled CDaam1 and 1 nM SNAP-649-CDaam1 (but lacking actin monomers) in TIRF buffer was introduced to the flow channel. Diffusion of single SNAP-649-CDaam1 molecules was recorded at high temporal resolution (670 ms). The gray line in the first frame represents the position of the actin bundle, and spots correspond to SNAP-649-CDaam1 molecules. The video is displayed at 50 fps. The movie corresponds to Figure 4E.

SUPPLEMENTAL EXPERIMENTAL PROCEDURES

Plasmids

E. coli expression plasmids for CDaam1 [1], human profilin [2], and fascin [3] have been described. Mammalian expression vectors for EGFP-FL-Daam1, EGFP-CDaam1 and EGFP-CDaam1ΔDAD were kind gifts from Raymond Habas (Temple University) [4]. To generate the SNAP-CDaam1 plasmid for expression and purification from yeast, the SNAP coding region of the SNAP-tag-T7-2-vector (New England Biolabs, Ipswich, MA, USA) was PCR amplified with a C-terminal GGSGGS flexible linker and subcloned into BglII/BamHI sites of pJM45, a 6xHis GAL1/10 *URA3* plasmid [5], producing a 6xHis SNAP GAL1/10 *URA3* plasmid (pCG105). Next, CDaam1 was subcloned into the BamH1/Not1 sites.

Cell culture, transfection, and RNAi silencing

Mouse cell lines (B16F1 melanoma, NIH3T3 fibroblast, N2A neuroblastoma, and Raw264.7 macrophages; ATCC, Manassas, VA, USA) were grown in DMEM (Gibco, Life technologies, Grand Island, NY, USA) supplemented with 10% fetal bovine serum (FBS) at 37°C and 5% CO_2. Cells were transfected with DNA and/or siRNA using Lipofectamine 2000 (Life Technologies, Grand Island, NY, USA). Briefly, siRNAs directed against human Daam1 mRNA coding region 5′-GGAAAGAGCAGGCAGAGAAUU- 3′ and 5′-AAGAGGAGGAGAGGAGUA- 3′ were used in combination to knockdown Daam1. To knockdown fascin, oligo Tc siRNA 5'-GUGGAGCGUGCACAUCGCC-3' was used as described [6]. Scramble siRNAs 5′-CAGUCGCGUUUGCGACUGG-3′ with dTdT overhangs at the 3′ terminus were used as controls. siRNA annealing was performed as described [7]. 120 hr post transfection, cells were either trypsinized for immunoblot analysis or plated for immunofluorescence on coverslips coated with 25 µM laminin (Life Technologies) before fixation. EGFP-FL-Daam1, EGFP-CDaam1 and EGFP-Daam1ΔDAD were transfected using Lipofectamine 2000, and transfection was confirmed by staining fixed cells with an anti-GFP antibody (MBL International Corp, Woburn, MA, USA).

Cell imaging

Cells were grown overnight on laminin-coated coverslips and then fixed with 4.0% para-formaldehyde in 1XPBS (2.7 mM KCl, 1.8 mM KH_2PO_4, 10 mM Na_2HPO4, 140 mM NaCl pH 7.4) for 30 min and treated for 30 min with permeabilization buffer (PBS, 100 mM glycine, and 0.1% Triton X-100). Cells were stained with primary antibodies (below) in buffer containing PBS, 0.05% (v/v) cold fish gelatin (Sigma-Aldrich, St. Louis, MO, USA) and 0.5% (w/v) bovine serum albumin (Sigma-Aldrich), then washed with PBS plus 0.1% Triton X-100, and treated with secondary antibodies. F-actin was stained with Rhodamine–phalloidin (R415, Life Technologies). Images were acquired using a Leica TCS SP5 DM6000 confocal microscope (Leica microsystems, Buffalo Grove, IL, USA) with a 100x HCX Plan APO 1.40 oil-immersion objective lens, and LCS software (Leica microsystems). Images were processed using Adobe Photoshop Element 3 (Adobe Systems Inc., San Jose, CA, USA).

Antibodies

Primary antibodies used in cell imaging, western blotting, and coimmunoprecipitations included: monoclonal α-Daam1 (ab56951; Abcam, Cambridge, MA, USA), monoclonal α-alpha-tubulin (DM1A, T9026; Sigma-Aldrich), polyclonal α-Daam1 (K-16, sc-55929; Santa Cruz Biotechnology Inc., Santa Cruz, CA, USA), monoclonal α-Fascin (55K-2,

Santa Cruz) and polyclonal α-GFP (598S; MBL International Corp). Rabbit polyclonal α-Daam1 antibody was a kind gift from Ray Habas [8]. Secondary antibodies included Alexa-fluor 633 donkey anti-rabbit (A21206; Life technologies) and Alexa-Fluor 488 donkey anti-goat (A21082; Life technologies).

Protein purification

Rabbit skeletal muscle actin was purified [9] and labeled with pyrenyl-iodoacetamide as described [10] or fluorescently labeled with Oregon-green as described [2]. Human profilin was purified as described [5]. Formin polypeptides were expressed as N-terminal 6XHis-fusions in *S. cerevisiae* [11] and purified as described [1, 11]. SNAP-649-mDia1 was prepared as described [12], except that a different dye (SNAP-DY649; New England Biolabs) was used for labeling. SNAP-CDaam1 was prepared as described [11] with minor modifications. Briefly, plasmids were transformed into yeast strain BJ2168, and 2 liters of cells were grown at 25°C in selective medium containing 2% raffinose to OD_{600} = 0.8. Then galactose (2% final) was added to induce expression, and cells were grown for another 12-16 hr. Cells were harvested by centrifugation and resuspended in a 3:1 (v/w) ratio of cells to water, drop-frozen in liquid nitrogen, mechanically lysed in a coffee grinder as previously described [11], and stored at -80°C until use. For each purification, 10 g of frozen lysed yeast powder was thawed at 1:3 (w/v) of 20 mM imidazole (pH 8.0), 2X PBS, 0.5% Nonidet P-40, 1 mM DTT, and protease inhibitors (final 1 mM phenylmethylsulfonyl fluoride and 0.5 µg/ml each of antipain, leupeptin, pepstatinA, chymostatin, and aprotinin). The 50 ml lysate was then centrifuged for 80 min in a Ti70 rotor (Beckman-Coulter, Fullerton, CA, USA) at 60,000 rpm and 4°C. The supernatant was harvested and mixed with 0.75 ml of Ni^{2+}-NTA-agarose beads (Qiagen, Valencia, CA, USA) and 20 µM SNAP-DY649, and rotated overnight at 4°C. To remove free dye, the beads were washed three times with 20 mM imidazole (pH 8.0), PBS, 1 mM DTT, 200 mM NaCl. Labeled SNAP-649-CDaam1 protein was eluted with 0.5 ml of 300 mM imidazole pH 8.0, 50 mM Tris pH 8.0, 100 mM NaCl, 1 mM DTT, 5% glycerol, then purified further on a Superose 6 gel filtration column (GE Healthcare, Pittsburgh, PA, USA) equilibrated in $HEKG_5$ buffer (20 mM Hepes (pH 7.5), 1 mM EDTA, 150 mM KCl, 5% glycerol). GST-fascin was expressed in *E. coli*, and frozen bacterial cell pellets were thawed and resuspended in PBS with 1 mM DTT and protease inhibitors, then lysed by treatment with lysozyme and sonication. Lysates were cleared by centrifugation at 60,000 rpm in a Ti70 rotor (Beckman/Coulter) for 30 min at 4°C. The supernatant was mixed with glutathione agarose (Qiagen, Valencia, CA, USA) for 1 hour at 4°C. Fascin was cleaved from GST by digestion with PreScission Protease (GE Healthcare), and the released protein was further purified on a Superose 6 gel filtration column (GE Healthcare) equilibrated in $HEKG_5$ buffer.

Actin assembly and bundling assays

For actin assembly assays, Ca^{2+}-ATP actin monomers (2 µM, 5% pyrene labeled) in G-buffer (10 mM Tris-Cl-, 0.1 mM $CaCl_2$, 0.2 mM DTT, and 0.2 mM ATP, pH 7.5) were converted to Mg^{2+}-ATP actin just before each reaction [11]. Actin was mixed with other proteins or control buffers, and polymerization was initiated by addition of 3 µL of 20X initiation mix (40 mM $MgCl_2$, 10 mM ATP, 1 M KCl). Pyrene fluorescence was monitored over time at excitation 365 nm and emission 407 nm at 25°C in a fluorimeter (Photon Technology International, Lawrenceville, NJ, USA). For low speed pelleting assays to detect actin filament bundling, monomeric actin (4 µM) was first polymerized for 1 h at 25°C in F-buffer (G buffer plus 1X initiation mix). Then the F-actin stock was diluted to 2.4 µM in $HEKG_5$ buffer in the absence or presence of different concentrations of formins to a final volume of 30 µL, and the filaments were gently pipetted using cut-off tips to

minimize shearing. After 10 min incubation at 25 °C, samples were centrifuged at 14,000 rpm for 5 min at 25 °C in a microcentrifuge (Eppendorf AG, Hamburg, Germany). The 30 µL supernatant was carefully removed, transferred to a new tube, and mixed with 15 µL of 3X SDS-PAGE sample buffer. The pellet was resuspended in 45 µL 1X SDS-PAGE sample buffer. Equivalent loads of supernatants and pellets were analyzed on Coomassie-stained SDS-PAGE gels.

TIRF microscopy and single molecule analysis

For TIRF microscopy, the preparation of biotin-polyethyleneglycol (PEG)-passivated cover slips, assembly of flow cells, image acquisition and image processing were performed as previously described [12]. Images were recorded using a Ti2000 inverted microscope (Nikon Instruments Inc., New York, NY, USA) equipped with a cooled, back-illuminated EMCCD camera (Andor Ixon, Belfast, Northern Ireland), a 150 mW Ar-laser (emission 488 nm) and a 15 mW HeNe-laser (emission 633 nm) (Mellot Griot, Carlsbad, CA, USA), both operated at maximum laser power in all experiments, and a Nikon CFI Apo TIRF 60x H objective. Before each reaction, 4 µg/mL streptavidin in 20 mM Tris-Cl− (pH 8.0), 1 mM DTT, 100 mM KCl was flowed in for 15 sec, followed by washing with 50 µl PBS + 1% BSA. The flow cell was then equilibrated with TIRF buffer (10mM imidazole (pH 7.4), 50 mM KCl, 1 mM $MgCl_2$, 1 mM EGTA, 0.2 mM ATP, 10 mM DTT, 15 mM glucose, 20 µg/ml catalase, 100 µg/ml glucose oxidase, and 0.5% methylcellulose (4000 cP)). For monitoring effects on actin polymerization, formins and/or other proteins as indicated were diluted into TIRF buffer, then rapidly mixed with 1 µM actin monomers (10% OG-labeled, 0.2% biotinylated) and introduced into the flow cell, which was then mounted on the microscope stage for imaging. Filament elongation rates were determined as described [12]. To monitor bundling effects of CDaam1 during actin polymerization, reactions were either performed as above in the presence of different concentrations of CDaam1 (50-200 nM) (Figure 2f, 2g), or 300 nM CDaam1 was flowed into the reaction chamber 10 min after initiation of actin polymerization (Figure 2i).

Single-molecule observations of SNAP-tagged formins on actin bundles was achieved using custom-made flow chambers assembled from a 60x24 mm, PEG-passivated coverslip attached to µ-Slide VI 0.4-adaptors (Ibidi GmbH, Martinsried, Germany) with a channel-volume of ~25 µl. Flow cells were washed with 50 µl PBS + 1% BSA, and equilibrated with TIRF buffer. Filament bundling in the flow channel was initiated by transferring a mixture of 1 µM actin (10% OG-labeled) and 300 nM fascin or CDaam1 in TIRF buffer into the chamber. For reactions containing CDaam1, 5 µM profilin was added to dampen additional nucleation events. Filaments were allowed to polymerize and bundle for 15 min, then 80 µl of a solution containing 300 nM untagged bundling protein and 1 nM SNAP-tagged formin (but lacking actin monomers) in TIRF buffer was introduced to the flow channel, replacing the previous reaction mixture. Flow-in was achieved using a syringe pump (Harvard Apparatus, Holliston, MA, USA), applying a flow rate of 100 µl/min. Images were recorded every 5 sec or, for tracking of the diffusion of single SNAP-649-CDaam1 molecules at high temporal resolution, every 665 ms. Image acquisition in all experiments was controlled by NIS-Elements software (Nikon Instruments Inc.).

Electron microscopy

For imaging actin filaments bundles, 25 µM Ca-ATP-G-actin in G-buffer (2 mM Tris, pH 7.4, 0.2 mM $CaCl_2$, 0.2 mM ATP, 0.2 mM DTT) was first mixed with 2 mM $MgCl_2$, 50 mM NaCl and polymerized at 25°C for 1 hour to reach steady state, and then stored on ice. 1 µM F-actin was incubated with or without 0.5 µM CDaam1 and/or 1 µM Fascin at 25°C

for 30 min. Alternatively, samples were incubated for 18 hours to obtain highly organized structures as previously described for fascin [13, 14]. Samples were diluted two fold in F-buffer (5 mM Tris, pH.7.4, 50mM NaCl, 2mM MgCl2, 0.2 mM EGTA, 1 mM DTT,) and applied to glow discharged formvar-carbon coated 200 mesh copper grids (Electron Microscopy Sciences, Hatfield, PA). Samples were adsorbed to grids for 30 sec, blotted to remove excess solution, negatively stained for 1 min with 2% (w/v) uranyl acetate (Electron Microscopy Sciences), blotted, and allowed to air-dry. Images were recorded with an AMT CCD camera on a FEI Morgani 268 transmission electron microscope (FEI, Hillsboro, OR) at an acceleration voltage of 80 kV and magnifications of 5600x and 22000x. Bundle widths (n >30 for each condition) were measured using the ruler tool in Adobe Photoshop by boxing a 2 micron long section of a bundle and dividing it into four even parts, then measuring the width for each section. Inter-filament distances and number of filaments per bundle (n >25 bundles) were measured using the Line scan tool of ImageJ software. The intensity profile of a line drawn across the bundle revealed a series of peaks corresponding to the individual filaments in the bundle. The distance between these peaks was used to measure the distance between filament centers.

Coimmunoprecipitations

B16F1 cells were grown to 70-90% confluency in 10 cm tissue culture dishes and transfected separately with plasmids expressing GFP, GFP-CDaam1, or GFP-FL-Daam1. After 48 hours, cells were trypsinized and lysed on ice in lysis buffer (50 mM Tris, pH 7.4, 150 mM NaCl, 0.1% Triton X-100, 0.2% NP-40, 4mM EDTA, 50 mM NaF, and 1 mM dithiothreitol) containing protease inhibitiors. Lysates were cleared by microcentrifugation at 14,000 rpm for 30 min at 4 °C. 300 µl of each lysate (equivalent protein concentrations verified by Bradford assay) were incubated with 15 µl of GFP-Trap_A beads (Chromotek, Planegg-Martinsried, Germany) for 2 hours on a rotator at 4 °C. Beads were then washed once with 100 µl of cold wash buffer (50 mM Tris, pH 7.4 and 0.1% Triton X-100), and equivalent loads of the input lysates and the pellet fractions were analyzed on immunoblots probed with α–fascin and α-GFP antibodies.

GST pull-down assays

Purified GST-fascin or GST alone was immobilized on glutathione-agarose beads (Sigma-Aldrich) in binding buffer (20 mM HEPES, pH 7.4, 50 mM KCl, 1 mM DTT). Beads were washed two times, then resuspended in 5 bead volumes binding buffer. Beads were mixed with soluble CDaam1 and incubated for 1 hour at 4°C. Final protein concentrations were 1 µM GST-fascin or GST, and 0.25 µM CDaam1. Beads were pelleted, supernatants were removed, and beads were washed two times in binding buffer. Pellets and supernatants were fractionated on SDS-PAGE gels, blotted, and probed with α-Daam1 antibodies (K16). Signals were quantified using ImageJ software (http://rsb.info.nih.gov/ij/).

Statistics and data analysis

All experiments were repeated at least two times and the Student t-test was used for statistical analysis. Kymographs of single-molecule binding events of SNAP-649-CDaam1 were obtained with the ImageJ plugin Multiple Kymograph (J. Rietdorf, FMI, Basel, Switzerland and A. Seitz, EMBL, Heidelberg, Germany). The mean-square displacement (MSD) of SNAP-649-CDaam1 diffusion along CDaam1-bundled actin filaments was calculated using Origin 8.0 software (OriginLab Corporation, Northampton, MA, USA). The diffusion coefficient was determined by linear regression of the MSD plotted against the time interval using the equation MSD = 2Dt (t=time in sec, D = diffusion coefficient in $\mu m^2 s^{-1}$).

SUPPLEMENTAL REFERENCES

1. Gould, C.J., Maiti, S., Michelot, A., Graziano, B.R., Blanchoin, L., and Goode, B.L. (2011). The formin DAD domain plays dual roles in autoinhibition and actin nucleation. Current biology : CB *21*, 384-390.
2. Kovar, D.R., Harris, E.S., Mahaffy, R., Higgs, H.N., and Pollard, T.D. (2006). Control of the assembly of ATP- and ADP-actin by formins and profilin. Cell *124*, 423-435.
3. Breitsprecher, D., Koestler, S.A., Chizhov, I., Nemethova, M., Mueller, J., Goode, B.L., Small, J.V., Rottner, K., and Faix, J. (2011). Cofilin cooperates with fascin to disassemble filopodial actin filaments. Journal of cell science *124*, 3305-3318.
4. Liu, W., Sato, A., Khadka, D., Bharti, R., Diaz, H., Runnels, L. W., and Habas, R. (2008). Mechanism of activation of the Formin protein Daam1. Proceedings of the National Academy of Sciences of the United States of America *105*, 210-215.
5. Moseley, J.B., Sagot, I., Manning, A.L., Xu, Y., Eck, M.J., Pellman, D., and Goode, B.L. (2004). A conserved mechanism for Bni1- and mDia1-induced actin assembly and dual regulation of Bni1 by Bud6 and profilin. Mol Biol Cell *15*, 896-907.
6. Vignjevic, D., Kojima, S., Aratyn, Y., Danciu, O., Svitkina, T., and Borisy, G.G. (2006). Role of fascin in filopodial protrusion. The Journal of cell biology *174*, 863-875.
7. Elbashir, S.M., Harborth, J., Lendeckel, W., Yalcin, A., Weber, K., and Tuschl, T. (2001). Duplexes of 21-nucleotide RNAs mediate RNA interference in cultured mammalian cells. Nature *411*, 494-498.
8. Sato, A., Khadka, D.K., Liu, W., Bharti, R., Runnels, L.W., Dawid, I.B., and Habas, R. (2006). Profilin is an effector for Daam1 in non-canonical Wnt signaling and is required for vertebrate gastrulation. Development *133*, 4219-4231.
9. Spudich, J.A., and Watt, S. (1971). The regulation of rabbit skeletal muscle contraction. I. Biochemical studies of the interaction of the tropomyosin-troponin complex with actin and the proteolytic fragments of myosin. The Journal of biological chemistry *246*, 4866-4871.
10. Pollard, T.D., and Cooper, J.A. (1984). Quantitative analysis of the effect of Acanthamoeba profilin on actin filament nucleation and elongation. Biochemistry *23*, 6631-6641.
11. Moseley, J.B., Maiti, S., and Goode, B.L. (2006). Formin proteins: purification and measurement of effects on actin assembly. Methods Enzymol *406*, 215-234.
12. Breitsprecher, D., Jaiswal, R., Bombardier, J.P., Gould, C.J., Gelles, J., and Goode, B.L. (2012). Rocket launcher mechanism of collaborative actin assembly defined by single-molecule imaging. Science *336*, 1164-1168.
13. Ishikawa, R., Sakamoto, T., Ando, T., Higashi-Fujime, S., and Kohama, K. (2003). Polarized actin bundles formed by human fascin-1: their sliding and disassembly on myosin II and myosin V in vitro. Journal of neurochemistry *87*, 676-685.
14. Jansen, S., Collins, A., Yang, C., Rebowski, G., Svitkina, T., and Dominguez, R. (2011). Mechanism of actin filament bundling by fascin. The Journal of biological chemistry *286*, 30087-30096.